

Reduction of N_3^- by $[\text{Mo}_2\text{Fe}_6\text{S}_8(\text{SPh})_9]^{3-}$ Modified Glassy Carbon Electrode—Model Study of Nitrogenase

Koji TANAKA,* Susumu KUWABATA, Satoshi DENNO, and Toshio TANAKA

Department of Applied Chemistry, Faculty of Engineering, Osaka University,
Yamada-oka, Suita, Osaka 565

(Received October 6, 1988)

The reduction of N_3^- by a $(\text{Bu}_4\text{N})_3[\text{Mo}_2\text{Fe}_6\text{S}_8(\text{SPh})_9]$ modified glassy carbon electrode has been conducted in a pH region 5 to 12 in water. In neutral and acidic conditions, N_3^- undergoes two- and six-electron reductions to afford not only N_2 and NH_3 but also N_2H_4 , and the total amounts of N_2 and N_2H_4 produced were essentially consistent with that of NH_3 . On the other hand, no N_2H_4 formation was observed in the pH region higher than 10, where an equal amount of N_2 and NH_3 was formed. The rate of N_2H_4 formation was linearly proportional to a concentration of N_3H , which exists as an equilibrium mixture with N_3^- in the aqueous phase, while that of N_2 evolution was controlled by the concentration of free N_3^- in H_2O . These observations indicate that N_2H_4 and N_2 result from the coordination of N_3H and N_3^- to the molybdenum-iron sulfur cluster, respectively.

Nitrogenase is composed of iron proteins and molybdenum-iron proteins and reduces not only N_2 but also various unsaturated small molecules such as C_2H_2 , N_3^- , RCN , RNC , and N_2O .¹⁾ Among those nitrogenase substrates, N_3^- is the only anionic substrate which is reduced with inequivalent numbers of electrons and protons. In the initial study on the reduction of N_3^- by crude nitrogenase in the presence of MgATP , N_3^- was reduced with two electrons to give an equal amount of N_2 and NH_3 .²⁾ Later, Hardy et al. have reported that the reduction of N_3^- afforded one N_2 molecule and two NH_3 molecules at low concentration of N_3^- , and the excess NH_3 has been attributed to result from the further reduction of the N_2 formed.³⁾ Furthermore, the formation of N_2H_4 in addition to N_2 and NH_3 was observed in the reduction of N_3^- by purified nitrogenase.⁴⁾ It has been argued whether N_3^- or N_3H is the actual substrate of nitrogenase^{2–5)} since both species exist as an equilibrium mixture around pH 7. Furthermore, N_3^- has been shown to disturb the electron flow in enzymatic reaction by inhibiting the rate of MgATP hydrolysis by nitrogenase.^{3,6)} Despite these difficulties, N_3H has been suggested to be a potent substrate for the formation of N_2H_4 based on the reduction of N_3^- conducted in a restricted pH range 6.5–7.3.⁷⁾

It has been demonstrated that various nitrogenase substrates such as C_2H_2 ,⁸⁾ CH_3CN ,⁹⁾ CH_3NC ,⁹⁾ and N_2O ¹⁰⁾ are reduced by the reduced species of $[\text{Fe}_4\text{S}_4(\text{SPh})_4]^{2-}$ and $[\text{Mo}_2\text{Fe}_6\text{S}_8(\text{SPh})_9]^{3-}$. One of the principal advantage of those model studies is that the reduction of nitrogenase substrates can be conducted in wide pH range, where proteins are readily denatured. The reduction of N_3^- by a model study, therefore, may give a clue to elucidate whether N_3^- or N_3H is the actual substrate of nitrogenase. The construction of a system which can not only rapidly but also continuously transport electrons to a catalyst having ability of multi-electron reduction of N_3^- is required in order to simulate the enzymatic reaction since N_3^- undergoes two-, six-, and eight-electron reductions by nitrogen-

ase.^{3,4)} This paper describes the reduction of N_3^- on a $(\text{Bu}_4\text{N})_3[\text{Mo}_2\text{Fe}_6\text{S}_8(\text{SPh})_9]$ modified glassy carbon electrode in H_2O .

Experimental

Commercially available guaranteed reagent grade of NaN_3 , H_3PO_4 , and NaOH were used without further purification. Water insoluble and soluble MoFeS clusters, $(\text{Bu}_4\text{N})_3[\text{Mo}_2\text{Fe}_6\text{S}_8(\text{SPh})_9]^{11)}$ ($(\text{Bu}_4\text{N})_3[\text{Mo-Fe}]$) and $(\text{Et}_4\text{N})_3[\text{Mo}_2\text{Fe}_6\text{S}_8(\text{SCH}_2\text{CH}_2\text{OH})_9]^{12)}$ and $(\text{Et}_4\text{N})\text{N}_3^{13)}$ were prepared according to the literature. Solvents used for electrochemical measurements were purified by distillation over appropriate desiccants; DMF from CaH_2 under reduced pressure and CH_3CN from P_2O_5 , and stored under N_2 atmosphere. Immediately before the electrochemical reduction of N_3^- , those solvents were bubbled with He at least for 1 h to remove nitrogen dissolved in the solvents. A $(\text{Bu}_4\text{N})_3[\text{Mo-Fe}]$ modified glassy carbon electrode was prepared by dropping a CH_3CN solution of $(\text{Bu}_4\text{N})_3[\text{Mo-Fe}]$ (1.0 mmol dm^{-3}) on a glassy carbon plates with areas 3.0 and 1.0 cm^2 (Tokai Carbon Co., Ltd., SC-2), and dried under N_2 atmosphere. The details of the cluster modified glassy carbon electrode was described in previous papers.^{10,14)}

Physical Measurements. Electronic absorption spectra were measured with a Union SM-401 spectrophotometer. Spectroelectrochemical experiments were carried out by the use of an optically transparent thin layer electrode.¹⁵⁾ Cyclic voltammetry was carried out by using a potentiostat (Hokuto Denko HA-301), a function generator (Hokuto Denko HB-107A), and an X-Y recorder (Yokogawa Electric Inc., 3077).

Reduction of N_3^- by the $[\text{Mo-Fe}]/\text{GC}$ Electrode. The reduction of N_3^- by the $[\text{Mo-Fe}]/\text{GC}$ electrode in water were carried out under the controlled potential electrolysis conditions using an electrolysis cell consisting of three components; a working, a counter, and an SCE reference electrode compartments.⁸⁾ A cation exchange membrane (Nafion film) was used as a separator between the working electrode and the counter electrode compartments. After passing He through the electrolysis cell for 1 h to remove air, an aqueous buffer solution (H_3PO_4 – NaOH) of NaN_3 was introduced into the working electrode compartment by syringe techniques. Then, the electrolysis cell was placed in a thermostat at 30 °C and the reduction of N_3^- was started by

applying a fixed potential to the [Mo-Fe]/GC electrode with a potentiostat. The charge consumed in the course of reduction was measured with a Hokuto Denko HF-201 coulometer. Analyses of H_2 and N_2 evolved in the reduction were conducted on a Shimadzu GC-3BT gas chromatograph with a 2.0 m column filled with Molecular Sieves 13X and on a Shimadzu GC-7A gas chromatograph with Porapack Q, respectively. Ammonia and N_2H_4 formed in solutions were determined by Shimadzu GC-6A gas chromatograph with Chromosorb 103 and by colorimetric titration,¹⁶ respectively.

Results and Discussion

Interaction of [Mo-Fe]³⁻ with N_3^- . The electronic absorption spectrum of $(n-Bu_4N)_3[Mo-Fe]$ in DMF shows two absorption bands at 360 and 460 nm (a broken line in Fig. 1), which did not change at all by addition of $(Et_4N)N_3$ to the solution. The electrochemical reduction of [Mo-Fe]³⁻ to [Mo-Fe]⁴⁻ at -1.10 V vs. SCE¹⁷ in DMF resulted in a decrease of the absorptivity at the 460 nm band (a dotted broken line in Fig. 1), while the electrochemical reduction of the cluster conducted in the presence of $(Et_4N)N_3$ under otherwise the same conditions leads to an appearance a new band at 306 nm (a solid line of Fig. 1). The 306 nm band can be assigned to PhS^- ^{14,18} dissociated from [Mo-Fe]⁴⁻, and the intensity of this band corresponds to one molecule of PhS^- per one molecule of the cluster. On the other hand, this band gradually disappeared by reoxidation of [Mo-Fe]⁴⁻ at -0.60 V vs. SCE, and the final spectrum became almost same as that of original [Mo-Fe]³⁻ in DMF. These results indicate that the oxidized cluster [Mo-Fe]³⁻ has no interaction with N_3^- , while a PhS^- ligand of [Mo-Fe]⁴⁻ is substituted by N_3^- to afford the 1:1 adduct. Such a substitution reaction may take place on the Fe atom of [Mo-Fe]⁴⁻ rather than the Mo atom, since a terminal RS^- is subject to a substitution

reaction, while the bridging RS^- ligands of the cluster are inert for substitutions.¹⁹

Cyclic Voltammograms of the [Mo-Fe]/GC Electrode. The cyclic voltammogram of the [Mo-Fe]/GC electrode in H_2O (pH 8) shows a cathodic wave around -1.25 V vs. SCE, followed by an irreversible cathodic current due to H_2 evolution catalyzed by the reduced species of the cluster, and an anodic wave around -0.75 V in the reverse scan (a dotted line in Fig. 2). Although the charge consumed in the cathodic process cannot be determined exactly due to the following irreversible cathodic current, that of the anodic one is just two electrons per a cluster modified on the glassy carbon plate. Thus, all the clusters modified on a glassy carbon plate undergo simultaneous two-electron reduction in water. The [Mo-Fe]^{3-/5-} redox cycle stably works on the glassy carbon plate since the cyclic voltammogram was essentially unchanged by successive potential scan at least for 2 h.¹⁴ The cathodic current density at more negative potentials than -1.1 V fairly increases by addition of NaN_3 (0.2 mol dm^{-3}) to the aqueous buffer solution at the same pH value (a solid line of Fig. 2). The threshold potential of the cathodic current in the presence of NaN_3 is essentially consistent with the reduction wave from [Mo-Fe]³⁻ to [Mo-Fe]⁵⁻ in the absence of NaN_3 , suggesting that the reduced forms of the cluster can effectively reduce N_3^- in water. The current density at more negative potentials than -1.1 V increases with decreasing the pH value (dotted broken and broken lines in Fig. 2).

Reduction of N_3^- by the [Mo-Fe]/GC Electrode.

As expected from the cyclic voltammograms of the

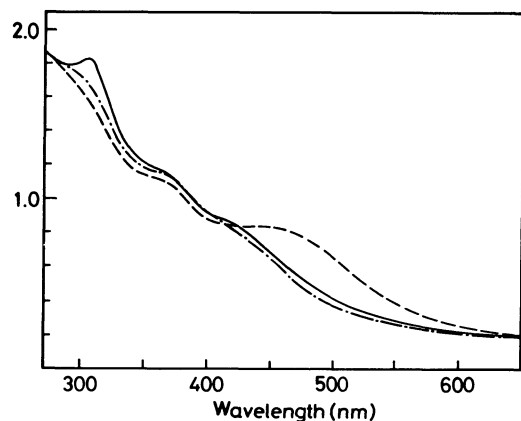


Fig. 1. Electronic absorption spectra of $(Bu_4N)_3[Mo_2Fe_6S_8(SPh)_9]$ ($4.0 \times 10^{-4} \text{ mol dm}^{-3}$) (-----) and the reduced species produced at -1.10 V vs. SCE in the absence (---) and the presence (— · —) of $(Bu_4N)N_3$ ($5.0 \times 10^{-2} \text{ mol dm}^{-3}$) in DMF.

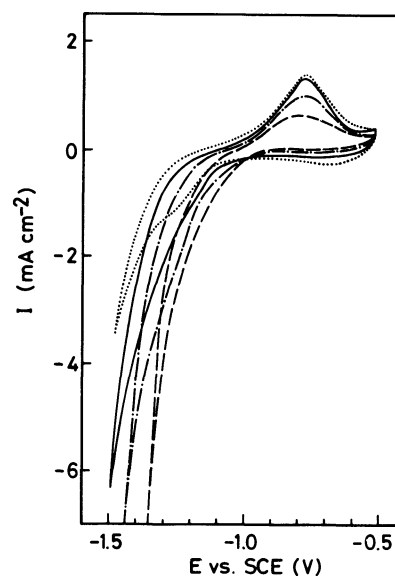
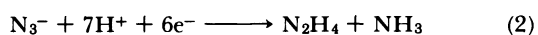
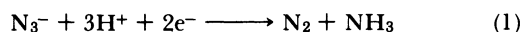


Fig. 2. Cyclic voltammograms of the [Mo-Fe]/GC electrode in H_2O (pH 8.0) in the absence (·····) and the presence of NaN_3 (0.2 mol dm^{-3}) in H_2O at pH 8.0 (—), 7.0 (— · —), and 6.0 (----): $dE/dt = 100 \text{ mV s}^{-1}$.

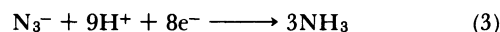
[Mo-Fe]/GC in the presence of NaN_3 at various pH, the reduction of N_3^- by the [Mo-Fe]/GC electrode at pH 6.0 is much faster than that at pH 12.0 under the controlled potential electrolysis at -1.25 V vs. SCE (Fig. 3). In addition, the reduction products are also altered by the change of pH; N_3^- is reduced to not only N_2 and NH_3 but also N_2H_4 at pH 6.0 (Fig. 3b), while only N_2 and NH_3 are formed in the same reduction at pH 12.0 (Fig. 3a). Thus, in acidic solutions both two- and six-electron reductions of N_3^- (Eqs. 1, 2) take place, and two-electron reduction of N_3^- (Eq. 1) occurs predominantly in



alkaline solutions. In order to elucidate such a pH dependency of the N_3^- reduction, reduction of N_3^- was conducted under various reaction conditions, and the results are summarized in Table 1.

The formation of N_2H_4 (Eq. 2) was observed in the pH less than 10 (Entries 1–7 in Table 1). The sum of the amounts of N_2 and N_2H_4 formed in that pH region

is essentially consistent with the amount of NH_3 , suggesting that N_2H_4 is not the precursor of NH_3 . In fact, N_2H_4 was not reduced by the [Mo-Fe]/GC electrode in H_2O under the present experimental conditions. Thus, the [Mo-Fe]/GC electrode can catalyze two- (Eq. 1) and six-electron (Eq. 2) reductions of N_3^- but has no ability to catalyze the eight-electron reduction of N_3^- (Eq. 3). The amounts of not only the



reduction products of N_3^- but also H_2 increase with decreasing the pH value of the aqueous phase. It should, however, be noticed that the amount of H_2 evolved are controlled by the potential of the [Mo-Fe]/GC electrode under a constant pH, while the amounts of N_2 , NH_3 , and N_2H_4 are not largely dependent on the electrode potential (Entries 2–4 in Table 1). The result indicates that H_2 evolution is controlled principally by the electron transfer from the GC plate to the cluster, and that the rate of the N_3^- reduction is governed mainly by the chemical reaction. Thus, the cluster modified on the glassy carbon plate effectively functions as a catalyst for the reduction of N_3^- . Holm et al. have reported that the reduced species of the present molybdenum-iron sulfur cluster has an

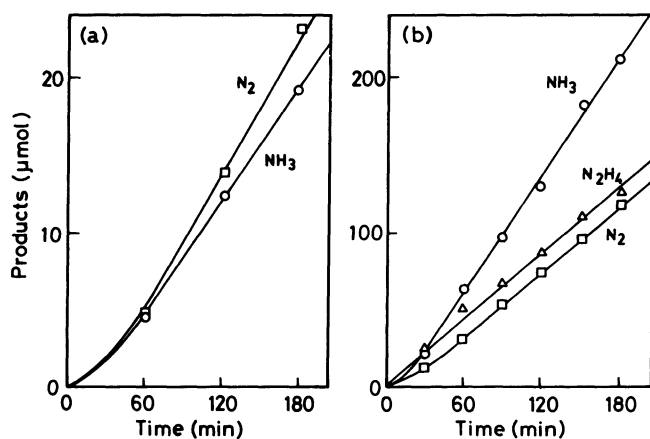


Fig. 3. Reduction of NaN_3 catalyzed by the [Mo-Fe]/GC under the controlled potential electrolysis at -1.25 V vs. SCE in H_2O at pH 12.0 (a) and 6.0 (b). The concentrations of NaN_3 are 0.5 mol dm^{-3} (a) and 0.05 mol dm^{-3} (b).

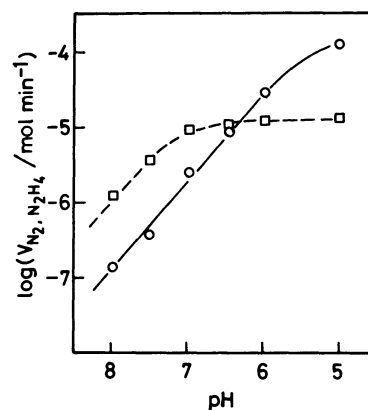


Fig. 4. Rates of the N_2H_4 (O) and N_2 (□) formation against pH of the electrolyte solutions in the reduction of NaN_3 (0.05 mol dm^{-3}) by the [Mo-Fe]/GC electrode at -1.25 V vs. SCE.

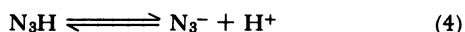
Table 1. The Reduction of N_3^- Catalyzed by the [Mo-Fe]/GC Electrode in H_2O for 150 min

Entry	NaN_3 mmol dm^{-3}	pH	E V vs. SCE	Products ^{a)}			
				NH_3	N_2	N_2H_4	H_2
1	50	5	-1.25	254	96	165	453
2	50	6	-1.10	179	92	89	16
3	50	6	-1.25	183	86	103	234
4	50	6	-1.40	188	89	95	1235
5	25	7	-1.25	49	23	28	77
6	50	7	-1.25	83	45	34	58
7	50	8	-1.25	3.6	3.2	0.3	51
8	50	10	-1.25	2.8	2.5	0	18.2
9	50	12	-1.25	1.3	1.3	0	1.1

a) μmol .

ability to reduce protons and metal-hydride species has been proposed as the precursor for the H_2 evolution.²⁰⁾ The difference of the rate determining steps in the reductions of protons and N_3^- by the [Mo-Fe]/GC electrode suggests that the reaction mechanisms of those two reactions are different from each other. The reduction of N_3^- may, therefore, be initiated by the coordination of N_3^- to the molybdenum-iron sulfur cluster modified on the GC plate since N_3^- is not reduced at all by a glassy carbon electrode at -1.25 V vs. SCE in H_2O .

As described above, the rates of N_2 and N_2H_4 formation²¹⁾ increased with decreasing pH values. The former, however, reaches a constant value below around 7 (a broken line in Fig. 4), and the latter also show the saturation behavior around 5 (a solid line in Fig. 4). Such a distinct difference in the formation rates between N_2H_4 and N_2 toward the pH change suggests that the reductions of Eqs. 1 and 2 take place independently. It is well-known that N_3^- exists as an equilibrium mixture with N_3H in H_2O , and the pK_a of N_3H is 4.6 at $30^\circ C$ (Eq. 4).²²⁾ The presence of the turning point in the plot of $\log V(N_2H_4)$ vs. pH ($V(N_2H_4)$: the rate of N_2H_4 formation) around pH 5 may, therefore, be associated with the pK_a . The concentrations of N_3H and N_3^- are expressed by Eqs. 5 and 6, where $[N_3^-]_0$ is the initial concentration of NaN_3 . Equations 5 and 6 also can be converted into Eqs. 7 and 8 in terms of pK_a and pH in place of



$$[N_3H] = [N_3^-]_0[H^+]/(K_a + [H^+]) \quad (5)$$

$$[N_3^-] = K_a[N_3^-]_0/(K_a + [H^+]) \quad (6)$$

$$[N_3H] = [N_3^-]_0/(10^{(pH-pK_a)} + 1) \quad (7)$$

$$[N_3^-] = 10^{(pH-pK_a)} [N_3^-]_0/(10^{(pH-pK_a)} + 1) \quad (8)$$

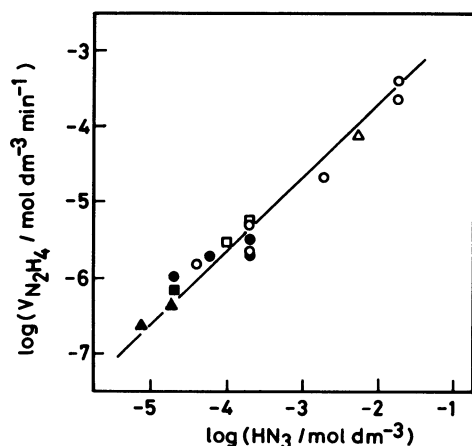
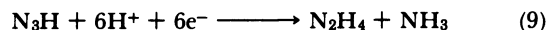


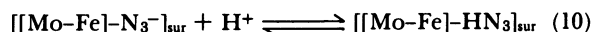
Fig. 5. Relationship between the rate of N_2H_4 formation and the N_3H concentration in the reduction of NaN_3 by the [Mo-Fe]/GC electrode at pH 6.0 (○), 6.5 (△), 7.0 (□), 8.0 (■), and 10.0 (▲).

K_a and $[H^+]$, respectively. Although any linear relationship was not observed between $\log V(N_2H_4)$ and $\log [N_3^-]$ calculated from Eq. 8, a plot of $\log V(N_2H_4)$ vs. $\log [N_3H]$ obtained from Eq. 7 gives a straight line, as shown in Fig. 5. A linear dependence of $V(N_2H_4)$ upon the N_3H concentration in the aqueous phase suggests that N_3H is the actual substrate for the formation of N_2H_4 . This conclusion may be supported by the fact that N_2H_4 is not produced above pH 10, where N_3H essentially does not exist as an equilibrium mixture of N_3^- . Equation 9 rather than Eq. 2 may,



therefore, be appropriate for the formation of N_2H_4 in the present study.

The saturation behavior of $\log V(N_2)$ around 7 (Fig. 4) also may be explained by a protonation equilibrium of the reaction intermediate. The reduction of N_3H formed in the aqueous phase may be initiated by the coordination of N_3H to the cluster on the [Mo-Fe]/GC, followed by the electron transfer to the N_3H from the cluster. It should be noticed that N_3^- also can coordinate to the reduced cluster but the rate of the electron transfer to the N_3^- from the cluster may be fairly slower than that to the N_3H ligated on the cluster since N_3^- is apparently much more basic than N_3H . Accordingly, smooth electron transfer from the cluster to the N_3^- coordinated may take place when the N_3^- undergoes a reversible protonation, as expressed by Eq. 10,



where $[[Mo-Fe]-N_3^-]_{sur}$ and $[[Mo-Fe]-HN_3]_{sur}$ are the cluster- N_3^- adduct and its protonated species, respectively, on the [Mo-Fe]/GC. The protonated cluster- N_3^- adduct ($[[Mo-Fe]-HN_3]_{sur}$) formed by the protonation (Eq. 10) is not necessarily the same species as the reaction intermediate involved in the reduction of N_3H affording N_2H_4 and NH_3 (Eq. 9) (vide infra). The proton dissociation constant pK'_a of $[[Mo-Fe]-HN_3]_{sur}$ (Eq. 10) may be fairly different from the pK_a of free HN_3 (Eq. 4; $pK_a=4.6$). As similar to Eq. 5, the surface concentration of $[[Mo-Fe]-HN_3]_{sur}$ of Eq. 10 can be expressed by Eq. 11,

$$[[Mo-Fe]-HN_3]_{sur} = [[Mo-Fe]-N_3^-]_0[H^+]/(K'_a + [H^+]) \quad (11)$$

where $[[Mo-Fe]-N_3^-]_0$ is the total surface concentration of the cluster- N_3^- adduct ($[[Mo-Fe]-N_3^-]_{sur}$) and its protonated species ($[[Mo-Fe]-HN_3]_{sur}$). As discussed in a previous section, the formation of H_2 , N_2 , and N_2H_4 takes place independently on the [Mo-Fe]/GC. To avoid an extreme difficulty in the determination of each surface concentrations of the active species in those reductions, the surface concentration of $[[Mo-$

$Fe]-N_3^-]_0$ is assumed to be proportional to the bulk concentration of N_3^- calculated from Eq. 8. The surface concentration of the cluster- N_3^- adduct ($[Mo-Fe]-N_3^-]_{sur}$ and its protonated species ($[Mo-Fe]-HN_3]_{sur}$), therefore, can be expressed in terms of $[N_3^-]$, K_a' , and $[H^+]$ (Eqs. 12, 13). On the basis of the fact

$$[Mo-Fe]-N_3^-]_{sur} \propto K_a' [N_3^-] / (K_a' + [H^+]) \quad (12)$$

$$[Mo-Fe]-HN_3]_{sur} \propto [N_3^-][H^+] / (K_a' + [H^+]) \quad (13)$$

that $V(N_2)$ is saturated around pH 7, a simulation fitting was conducted in the plots of $\log V(N_2)$ vs. $\log [Mo-Fe]-N_3^-]_{sur}$ and $\log [Mo-Fe]-HN_3]_{sur}$ by changing K_a' value around 10^{-7} . The best result was obtained at K_a' is $10^{-6.8}$ in the plot of $\log V(N_2)$ vs. $\log [Mo-Fe]-HN_3]_{sur}$, where the rate of N_2 formation in the reduction of N_3^- under various conditions shows a linear dependence on the calculated value $[N_3^-][H^+] / (K_a' + [H^+])$, as shown in Fig. 6, suggesting that $[Mo-Fe]-HN_3]_{sur}$ selectively affords N_2 and NH_3 (Eq. 1). The large pK_a' value (6.8) of $[Mo-Fe]-HN_3]_{sur}$ compared with the pK_a value (4.6) of N_3H in water can be explained by an increase in the electron density of N_3^- moiety upon the coordination to the cluster. Such an enhancement of the basicity of N_3^- may be caused by electron transfer through the terminal nitrogen atom bonded to the cluster, since N_3^- usually coordinates to metal complexes with a terminal nitrogen.²³ The initial protonation of N_3^- ligated on the cluster may, therefore, take place on the nitrogen atom bonded to the cluster to produce $[Mo-Fe]-HN-N=N$ (1) rather than $[Mo-Fe]-N=N-NH$ (2). The structure of 1 seems to explain reasonably the dissociation of the terminal N_2 moiety upon further protonation coupled with electron transfer from the cluster to $HN-N=N$ moiety. In accordance with this, protonation of $M-N_3^-$ complexes ($M=Ru$,²⁴ Co ,²⁵



Scheme 1.

Ir^{26}) also occurs at the nitrogen atom bonded to the metal, followed by the dissociation of terminal N_2 .

The protonation of N_3^- in a solution has been shown to occur at one of a terminal nitrogen atom of N_3^{27} (Scheme 1). The linear dependence of the rate of N_2H_4 formation upon the concentration of N_3H in the aqueous phase (Eq. 4) indicates the appropriateness of Eq. 9. In contrast to the protonation of $[Mo-Fe]-\bar{N}=\bar{N}=\bar{N}$ affording $[Mo-Fe]-HN-\bar{N}=\bar{N}$ (1), N_3H may bind to the cluster with the nonprotonated terminal nitrogen atom affording $[Mo-Fe]-\bar{N}=\bar{N}=NH$ (2) rather than 1. The intramolecular electron transfer from the cluster to the N_3H moiety of 2 may cause also the increase of the basicity of the nitrogen atom bonded to the cluster, resulting in further protonation to form $[Mo-Fe]-NH-N=NH$ (3). The following electron transfer coupled with protonation of 3 may lead the dissociation of N_2H_4 . It should be noticed that such the six-electron reduction of N_3^- (Eq. 2) hardly took place under the controlled potential electrolysis of an aqueous solution (pH 7.0, 12 cm³) containing $(Et_4N)_3[Mo_2Fe_6S_8(SCH_2CH_2OH)_9]$ (0.37 mmol dm⁻³) and NaN_3 (0.37 mol dm⁻³) at -1.25 V vs. SCE, where the two-electron reduction of N_3^- (Eq. 1) predominantly occurred with concomitant H_2 evolution. The mole ratios of N_2 and H_2 to NH_2NH_2 formed in this homogeneous system were 25 and 194, respectively, and the turnover number for the formation of N_2H_4 was as low as 0.385/h based on the amount of the cluster. On the other hand, the $[Mo-Fe]/GC$ catalyzes the six-electron reduction of N_3^- affording N_2H_4 with the turnover number 235/h under the same electrolysis potential at pH 7 (Entry 6 in Table 1). Despite that both $[Mo_2Fe_6S_8(SPh)_9]^{3-}$ and $[Mo_2Fe_6S_8(SCH_2CH_2OH)_9]^{3-}$ similarly undergo two successive one-electron reduction at more positive potentials than -1.25 V in solutions, the outstanding ability of the former modified glassy carbon electrode for the six-electron reduction of N_3^- may be explained by the view that the cluster of the $[Mo-Fe]/GC$ exists as the reduced form even after two-electron reduction of N_3^- due to fast and continuous electron transport to $[Mo_2Fe_6S_8(SPh)_9]^{3-}$ from the glassy carbon plate. This assumption is supported by the fact that the cyclic voltammogram of the $[Mo-Fe]/GC$ clearly exhibits the anodic wave of the cluster even in the presence of N_3^- (Fig. 2). Thus, the system which is provided with rapid and continuous electron transport to a redox catalyst may be one of the essential factor to catalyze a multi-electron reduction involving unstable reaction intermediates.

The reduction of N_3^- by nitrogenase affords also N_2 , NH_3 , and N_2H_4 around pH 7, and the amount of NH_3 has been shown to be larger than the total amount of

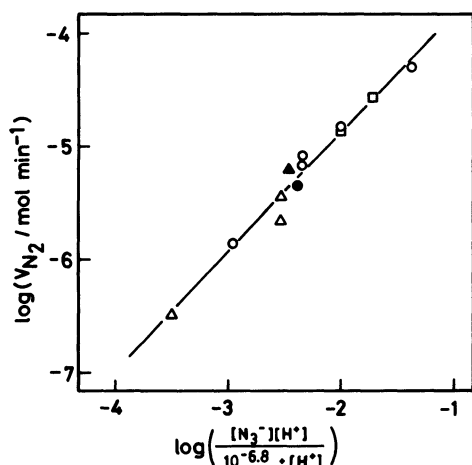


Fig. 6. Relationship between the rate of N_2 formation and $\log ([N_3^-][H^+] / (10^{-6.8} + [H^+]))$ in the reduction of NaN_3 by the $[Mo-Fe]/GC$ electrode at pH 6.0 (O), 6.5 (Δ), 7.0 (\square), and 10.0 (\blacktriangle).

N₂ and N₂H₄. This has been ascribed to further six-electron reduction of N₂ formed in the two-electron reduction of N₃⁻. The [Mo-Fe]/GC electrode has no ability of catalyzing the eight-electron reduction of N₃⁻ though the [Mo-Fe]/GC reasonably explains the difference in the two- and six-electron reduction of N₃⁻ in a wide pH range.

References

- 1) H. Dalton and L. E. Mortenson, *Bacteriol. Rev.*, **1972**, 231. L. E. Mortenson and R. N. F. Thorneley, *Ann. Rev. Biochem.*, **48**, 387 (1979).
- 2) R. Schollhorn and R. H. Burris, *Proc. Natl. Acad. Sci. U.S.A.*, **57**, 1317 (1967).
- 3) R. W. F. Hardy and E. Knight, Jr., *Biochim. Biophys. Acta*, **139**, 69 (1967).
- 4) M. J. Dilworth and R. N. F. Thorneley, *Biochem. J.*, **193**, 971 (1981).
- 5) J. -G. Li, B. K. Burgess, and J. L. Corbin, *Biochemistry*, **21**, 4393 (1982). T. E. Hermann and P. W. Wilson, *J. Bacteriol.*, **126**, 743 (1976).
- 6) T. Lijones, *Biochim. Biophys. Acta*, **321**, 103 (1973).
- 7) J. F. Robinson, B. K. Burgess, J. L. Corbin, and M. J. Dilworth, *Biochemistry*, **24**, 273 (1985).
- 8) R. S. McMillan, J. Renaud, J. G. Reynolds, and R. H. Holm, *J. Inorg. Biochem.*, **11**, 213 (1979). K. Tanaka, M. Honjo, and T. Tanaka, *ibid.*, **22**, 187 (1984).
- 9) K. Tanaka, Y. Imasaka, M. Tanaka, M. Honjo, and T. Tanaka, *J. Am. Chem. Soc.*, **104**, 4258 (1982).
- 10) S. Kuwabata, S. Uezumi, K. Tanaka, and T. Tanaka, *Inorg. Chem.*, **25**, 3018 (1986).
- 11) G. Christou, C. D. Garner, and R. M. Miller, *J. Chem. Soc., Dalton Trans.*, **1980**, 2363.
- 12) G. Christou, C. D. Garner, F. E. Mabbs, and M. G. B. Drew, *J. Chem. Soc., Chem. Commun.*, **1979**, 91.
- 13) R. E. Palermo, R. Singh, J. K. Bashkin, and R. H. Holm, *J. Am. Chem. Soc.*, **106**, 2600 (1984).
- 14) D. Lexa, J. M. Savent, and J. Zickler, *J. Am. Chem. Soc.*, **99**, 2786 (1977).
- 15) S. Kuwabata, K. Tanaka, and T. Tanaka, *Inorg. Chem.*, **25**, 1691 (1986).
- 16) G. W. Watt and J. Chrips, *Anal. Chem.*, **24**, 2066 (1952).
- 17) G. Christou, P. K. Mascharak, W. H. Armstrong, G. Papaefthymiou, R. B. Frankel, and R. H. Holm, *J. Am. Chem. Soc.*, **104**, 2820 (1982).
- 18) K. Tanaka, M. Moriya, S. Uezumi, and T. Tanaka, *Inorg. Chem.*, **27**, 137 (1988).
- 19) R. E. Palermo, P. P. Power, and R. H. Holm, *Inorg. Chem.*, **21**, 173 (1982).
- 20) T. Yamamura, G. Christou, and R. H. Holm, *Inorg. Chem.*, **22**, 939 (1983).
- 21) An induction period was observed for the formation of N₂ and N₂H₄ in the reduction of N₃⁻ by the [Mo-Fe]/GC electrode in H₂O. So the rates of the N₂ and N₂H₄ formation were obtained after 30 min, where both products linearly were produced with time (Fig. 3).
- 22) J. H. Boughton and R. N. Keller, *J. Inorg. Nucl. Chem.*, **28**, 2851 (1966).
- 23) Z. Dori and R. F. Ziolo, *Chem. Rev.*, **73**, 247 (1973).
- 24) L. A. P. Kane-Maguire, P. S. Sheridan, F. Basolo, and R. G. Person, *J. Am. Chem. Soc.*, **92**, 5685 (1970).
- 25) F. Monacelli, G. Mattogno, D. Gattegno, and M. Matese, *Inorg. Chem.*, **9**, 686 (1970).
- 26) B. C. Lome, J. W. McDonald, F. Basolo, and R. G. Person, *J. Am. Chem. Soc.*, **94**, 3786 (1972).
- 27) A. Mertens, K. Lammertsma, M. Arvanaghi, and G. A. Olah, *J. Am. Chem. Soc.*, **105**, 5657 (1983).